Proceedings of the International Gas Turbine Congress 2003 Tokyo
November 2-7, 2003

IGTC2003Tokyo TS-119

Development of a Next-Generation Ni-base Single Crystal Superalloy

Yutaka KOIZUMI,[1] Toshiharu KOBAYASHI,[1] Zhang JIANXIN,[1] Tadaharu YOKOKAWA,[1] Hiroshi HARADA,[1]
Yasuhiro AOKI,[2] and Mikiya ARAI[2]

[1]High Temperature Materials Group,
National Institute for Materials Science (NIMS)
1-2-1 Sengen, Tsukuba Science City, Ibaraki 305-0047, Japan
Phone: +81-29-859-2521; FAX: +81-29-859-2501; E-mail: koizumi.yutaka@nims.go.jp
[2]Materials Technology Department
Aeroengine & Space Operations
Ishikawajima-Harima Heavy Industries (IHI), Japan

ABSTRACT

In the context of the "High Temperature Materials 21 Project" conducted by NIMS, June 1999 - March 2006, we are developing superior Ni-base superalloys for turbine blades and vane materials. The designs are for high-efficiency gas turbines and next generation aeroengines.

Based on a fourth generation SC superalloy, TMS-138, we designed a new alloy that contains a higher amount of Mo to make the lattice misfit larger in the negative ($a\gamma' < a\gamma$), with the expectation that a finer dislocation network would be generated. The Ru content was also increased to improve the phase stability. The creep strength and microstructure of this alloy were examined and compared with those of the base alloy TMS-138 and a third generation SC superalloy, CMSX-10.

As predicted by our alloy design program, TMS-162 possesses excellent creep properties. The time to 1% creep deformation at 1100°C/137MPa was about 2.5 times as long as that of TMS-138 and 5 times as long as that of CMSX-10. The temperature capability of TMS-162 has reached the project target of 1100°C under stress at 137MPa and a creep rupture life as long as 1000 h, which constitutes a world record.

INTRODUCTION

The most effective approach to improve thermal efficiencies of aeroengines and industrial gas turbines is to increase the turbine inlet gas temperatures. To achieve higher temperatures, nickel (Ni)-base superalloys with higher temperature capabilities have been desired (Harada, 2000) since the invention of gas turbines.

In the latest civil aeroengines, for instance, so-called third generation single crystal (SC) superalloys CMSX-10 (RR3000) and the modified alloy CMSX-10+ (RR3010) have been used for uncooled intermediate-pressure blades (Erickson, 1996) whose metal temperatures can rise above 1000°C at takeoff. These alloys contain up to 6 wt% rhenium (Re) to improve the creep strength. However, the total amount of strengthening elements, including Re, has been beyond the solubility limit and, consequently, after long-term exposure at high temperatures, a significant amount of detrimental phases, so-called topologically close-packed (TCP) phases, containing high Re and other strengthening elements, form to reduce the creep strength. This limits the actual durability of the components. In addition, for the design of next-generation aeroengines for the Airbus 380 and Boeing 7E7, new SC superalloys with higher temperature capabilities will be required.

In the "High Temperature Materials 21 Project" conducted by NIMS, June 1999 - March 2006, we have been developing new SC superalloys with superior microstructural stabilities as well as creep strengths; the target temperature capabilitiy is 1100°C under stress at 137MPa and creep rupture times as long as 1000 h (Harada, 2002). We have reached 1083°C with a fourth generation SC alloy, TMS-138 (Koizumi et al., 2001; Zhang et al., 2002); however, the target has not been achieved.

In this study, we are developing a next generation SC superalloy that meets the target for achieving new aeroengines and advanced industrial gas turbines with very high thermal efficiencies.

Manuscript Received on Semtember 9, 2003

Table 1. Chemical compositions (wt% Ni-bal.) of the three alloys examined in this study.

	Co	Cr	Mo	W	Al	Ti	Nb	Ta	Hf	Re	Ru
CMSX-10	3.3	2.4	0.4	5.3	5.7	0.2	0.08	8.2	0.03	6.3	-
TMS-138	5.8	2.8	2.9	6.1	5.8	-	-	5.6	0.05	5.1	1.9
TMS-162	5.8	2.9	3.9	5.8	5.8	-	-	5.6	0.09	4.9	6.0

ALLOY DESIGN

A new SC superalloy was designed using a fourth generation SC superalloy, TMS-138, as a base alloy. According to the calculations by our alloy design computer program, an increased amount of Mo was added to strengthen the alloy. As Mo is partitioned more to the γ phase rather than the γ' phase and the atomic volume of Mo is larger than that of Ni (Yokokawa et al., 2002), the addition of Mo increases the γ lattice parameter rather than γ' (Zhang et al., 2002), changing the lattice misfit towards a larger negative. Here, the lattice misfit, δ, is expressed as, $\delta = (a\gamma' - a\gamma) / a\gamma$; aγ and aγ' are the lattice parameters of γ and γ' phases, respectively. A larger negative lattice misfit is known to enhance rafting, and also a formation of finer interfacial misfit dislocation network, both are known to improve the alloy creep strength (Zhang et al., 2002). Mo addition, however, normally decreases the phase stability, and the alloy becomes TCP-prone. To suppress the possible TCP formation, all the platinum group metal additions were found to be effective, and, for the present work, ruthenium (Ru) was added. It has been reported in our previous paper (Koizumi et al., 2001) that a Ru addition itself does not improve the creep strength at 1100°C /137MPa but simply improve the phase stability. The alloy composition thus designed is presented in Table 1 with those of alloys TMS-138 and CMSX-10.

EXPERIMENTAL PROCEDURE

SC bars of 10 mm diameter and 130 mm length of the designed alloy, TMS-162, and the base alloy, TMS-138, were cast in a NIMS directionally solidification (DS) furnace with 2 kgs of the remeltbars. The mold withdrawal rate, which corresponds to the solidification rate, was 200 mm/h for both.

The heat treatment condition of TMS-162 was selected by microstructure examination after heating small slices of the SC samples at various temperatures ranging from 1280 to 1360°C for 2 h. The solution treatment window of TMS-162 was found to be as large as 40°C, ranging from 1310 to 1350 °C. Thus, 1330°C was selected as the optimum temperature for the solution treatment.

Actual heat treatment of the creep specimens was performed in argon (Ar) gas-sealed quartz tubes. After 1 h heating at 1310°C, the samples were heated to 1330°C, held for 5 h, and then air-cooled. A two-step aging treatment was performed, first at 1000°C for 4 h, followed by air-cooling, and second at 870°C for 20 h, followed by air-cooling. From the fully heat-treated SC bars of longitudinal axes within 10 degrees of the <001> direction, creep specimens of 4 mm diameter and 20 mm length as gage part were machined out and carefully finished by grinding. For TMS-138 and CMSX-10, proper heat treatments were performed before machining creep specimens to the same shape.

Creep tests were carried out at 1100°C/137MPa and 800°C/735MPa. At 1100°C/137MPa, a non-contact creep strain-measuring device was used to obtain precise creep curves. Microstructures, especially the dislocation structures in creep ruptured samples, were examined using a Transmission Electron Microscope (TEM).

RESULTS AND DISCUSSION

Creep Property

Creep curves obtained at 1100°C/137MPa are presented in Fig. 1. It is clearly shown that the newly designed alloy TMS-162 has the longest creep rupture life, which is about 3 times as long as that of CMSX-10 and 2.5 times as long as that of TMS-138. When a comparison is made in time to the 1% creep, the advantage is even more significant; the time is about 5 times as long as that of CMSX-10 and 2.5 times as long as that of TMS-138. The corresponding creep rate vs. time curves are presented in Fig. 2. This figure clearly shows that the minimum creep rate becomes smaller in the order of CMSX-10, TMS-138, and TMS-162, while the time to reach the minimum creep rate is the shortest with CMSX-10 (about 3% of creep life) and the longest with TMS-162 (40%). Also, interestingly, the initial creep rate is the largest with TMS-162, but the creep rate decreases with time and reaches the lowest rate, exhibiting the longest creep life among the three alloys.

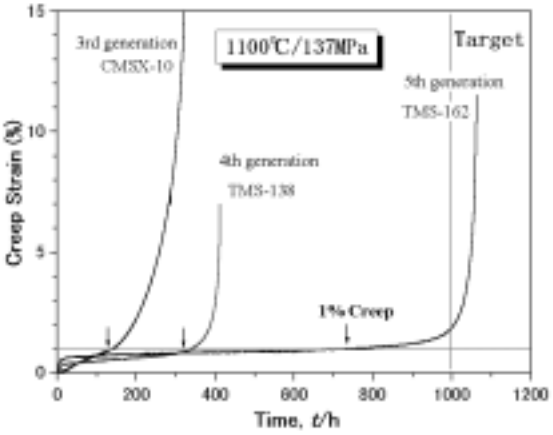

Fig.1 Creep strain - testing time curves at 1100℃/137MPa of three alloys, CMSX-10, TMS-138 and TMS-162.

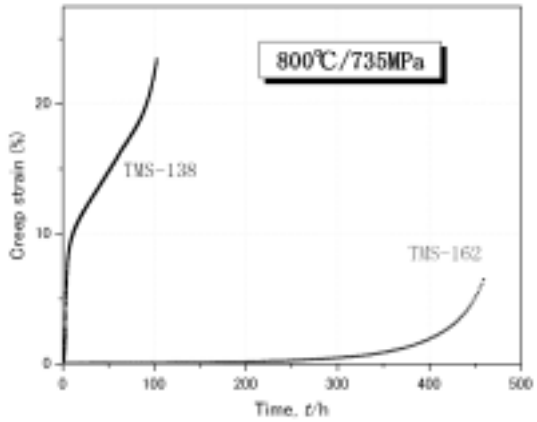

Fig. 3 Creep strain - testing time curves at 800℃/735MPa of alloys TMS-138 and TMS-162.

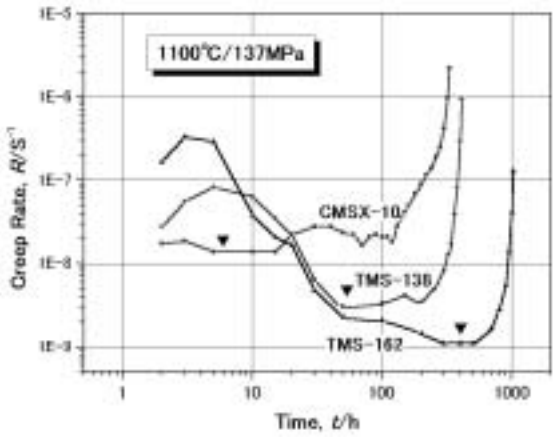

Fig. 2 Creep rate-time curves of three alloys of CMSX-10, TMS-138, and TMS - 162 at 1100℃/137MPa.

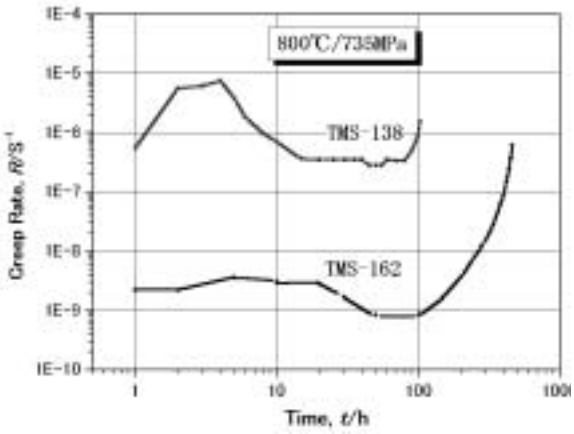

Fig. 4 Creep rate - time curves of alloys TMS-138 and TMS-162 at 800℃/735MPa.

TMS-138 has the same tendency, but it is not as significant as that of TMS-162.

This unique change in the creep rate is due to the so-called rafting of the γ/γ' structure. The same tendency as we see in TMS-138 and TMS-162 has been observed in other SC superalloys, i.e., TMS-82+ (second generation SC alloy) and TMS-75 (third generation SC alloy) (Hino et al., 2000), and it has become clear that rafting is responsible for this; during rafting, the creep rate increases, but the creep rate starts to decrease as the rafted structure is completed (Mackay et al., 1984). TMS-162 and TMS-138 seem to follow the same procedure.

The creep rupture strength of TMS-162 meets the “High Temperature Materials 21 Project” target, that is, 1000 h of rupture life at 1100°C/137MPa. This is the first Ni-base SC superalloy that ever reached a temperature capability of 1100°C under this condition.

At a lower temperature and higher stress creep condition simulating a blade root part, TMS-162 again had high strength, as presented in Fig. 3, whereas the fourth generation SC alloy TMS-138 showed about 10% initial creep followed by a fast secondary creep deformation to rupture. The creep rate of the alloys is also presented in Fig. 4. TMS-162 has more than two-orders smaller creep rate than TMS-138.

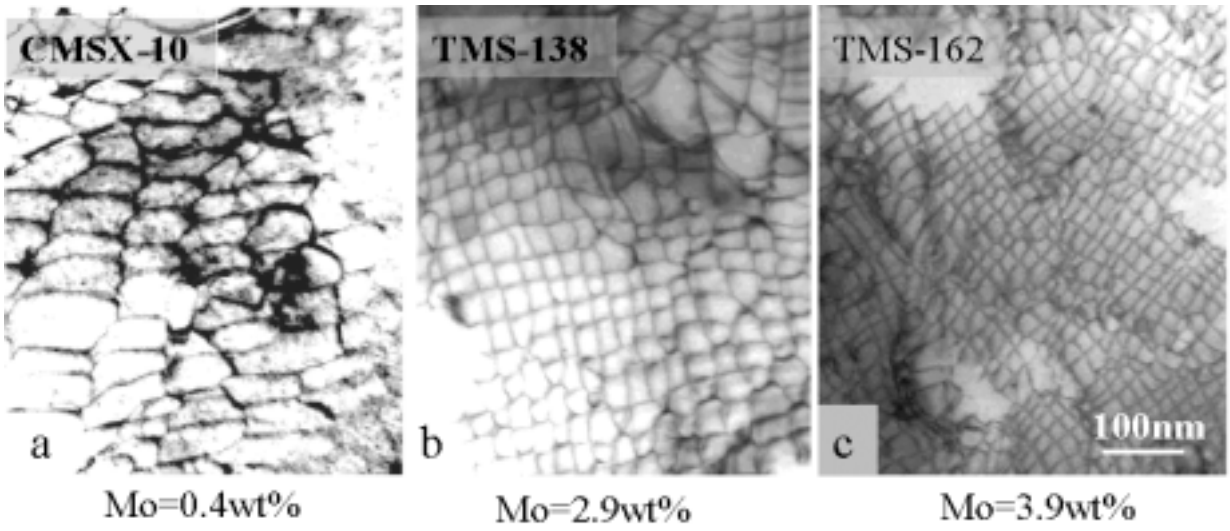

Fig.5 Transmission electron micrographs of the creep ruptured alloy of CMSX-10(a),TMS-138(b) and TMS-162(c),showing the difference in the interface dislocation networks among three ruptured alloys.

TEM Observation of the Creep-ruptured Samples

TEM observations were made with CMSX-10, TMS-138, and TMS-162 samples creep-ruptured at 1100°C/137MPa.

The observations were made at about 6 mm distance from the fractured surface, where little effect of necking caused by tertiary creep deformation is expected and, consequently, the rafted structure built up during secondary creep is well preserved. It was found that the rafted structure is less perfect in CMSX-10, whereas very well rafted structures were observed in both alloys TMS-138 and TMS-162.

By the observation, as shown in Fig. 5, we also found dislocation network generated on the rafted γ/γ' interface perpendicular to the stress axis near <001>. The dislocation network is also preserved during cooling after the creep rupture because of its nature; the dislocations restrain each other and also need climbing to move. The dislocation network becomes finer in the order of CMSX-10, TMS-138, and TMS-162. When the lattice misfit becomes larger in the negative, the interfacial dislocation network becomes finer to relieve the coherency strain. The difference in the dislocation spacing observed in Fig. 5 is attributed to the difference in the lattice misfit mainly due to the difference in the Mo content as designed.

The minimum creep rate at 1100°C/137MPa is plotted against the mean dislocation spacing in Fig. 6. There is a linear relationship between logarithms of the minimum creep rate and the dislocation spacing. As the Mo amount increases

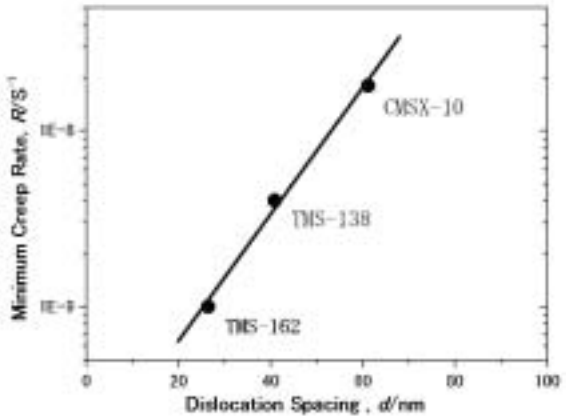

Fig. 6 Minimum creep rates of CMSX-10, TMS-138 and TMS-162 as a function of their interfacial dislocation spacing.

and the γ/γ' interfacial dislocation network becomes finer, the minimum creep rate decreases greatly. The same relationship has been reported in previous papers by some of the authors of the present paper and their coworkers (Hino et al., 2000, Zhang et al., 2002).

During creep at a higher temperature and a lower stress condition such as 1100°C/137MPa, the rafted structure is ideally built up especially when the lattice misfit is large in negative, and the γ channel parallel to the stress axis almost

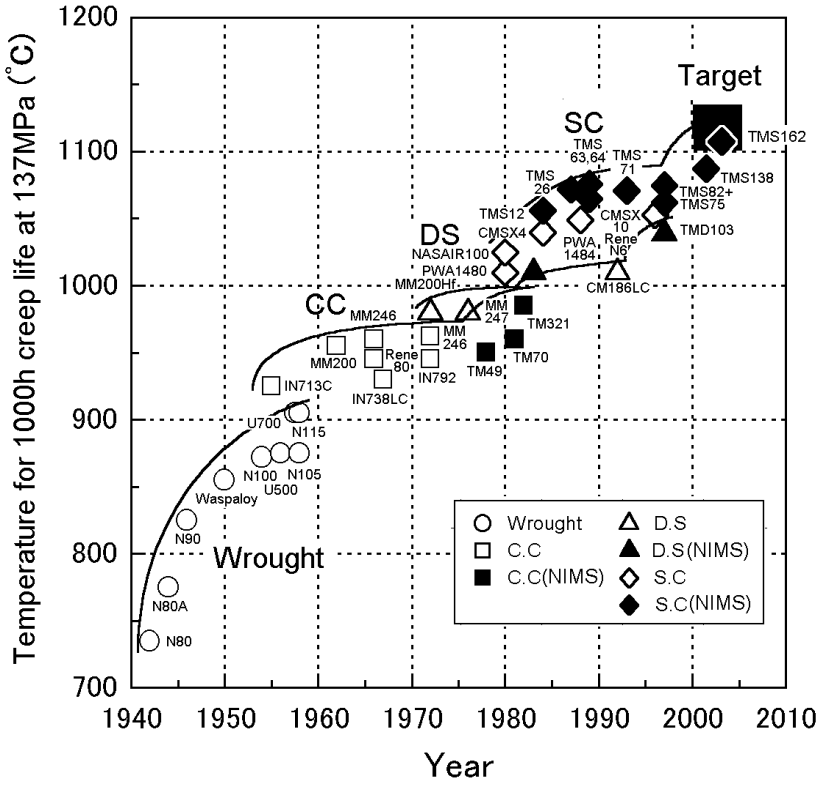

Fig. 7 History of improvement in temperature capability of Ni-base superalloys.

disappears. As a result, dislocation climbing along the longitudinal direction becomes very difficult. This is why the creep rate decreases when the rafted structure is built up. In this situation, as an alternative way for the gliding dislocations to move, they start cutting into the γ' phase as superdislocations (Caron et al., 1983). Here, the γ/γ' interfacial dislocation network effectively prevents the dislocation cutting into γ' because the gliding dislocations must pass through the dislocation network. The stress, τ, needed for a dislocation to bow out of the network is expressed as, $\tau = \alpha Gb/R$, where α is a constant value, G is the shear stress, b is Barger's vector, and R is the radius of the dislocation bowing out (Nabarro et al., 1995). As the network becomes finer, the R becomes smaller, and τ becomes larger. This means that a higher shear stress is needed for the dislocation to pass through a finer dislocation network, which resulted in the relationship shown in Fig. 6. The remarkable creep strength of TMS-162 is thus attributed to the fine dislocation network generated on the γ/γ' interfaces as well as the ideally built up rafted structure.

Figure 7 presents a history of the improvement in the temperature capability of Ni-base superalloys. TMS-162 is plotted at 1102°C, which is the world's highest temperature capability ever reached with SC superalloys.

CONCLUSIONS

Based on a fourth generation SC superalloy TMS-138, we designed a new alloy containing a higher amount of Mo to make the lattice misfit larger in the negative ($a\gamma' < a\gamma$), with the expectation that a finer dislocation network would be generated. The Ru content was also increased to improve the phase stability. The creep strength and microstructure of this alloy were examined, and the following conclusions were reached.

(1) The developed alloy TMS-162 has a time to 1% creep deformation at 1100°C/137MPa, about 2.5 times as long as that of TMS-138 and 5 times as long as that of CMSX-10, which is the third generation SC superalloy used in practice.

(2) There is a clear relationship between the γ/γ' interfacial

dislocation network spacing and the minimum creep rate. As the spacing becomes finer, the creep rate drastically decreases.

(3) TMS-162 with an increased Mo content, which creates a large negative lattice misfit, has the finest dislocation network on the γ/γ' interfaces in a very well rafted structure; this resulted in the longest creep life.

(4) The temperature capability of TMS-162 has reached the "High Temperature Materials 21 Project" target of a temperature capability of 1100°C under stress at 137MPa and a creep rupture life as long as 1000 h. This temperature capability is the highest ever reported in the world.

Acknowledgements

The authors express their sincere thanks to Mr. S. Masaki of Ishikawajima Precision Castings and Mr. M. Hosoya of Ishikawajima Harima Heavy Industries for their invaluable suggestions. Mr. H. Miyashiro, Mr. M. Kadoi, and Mr. S. Nakazawa are also acknowledged for their support with the experiments.

References

Harada H., 2000, *Journal of the Gas Turbine Society of Japan* 28 (2000) 278-284.

Erickson G.L., 1996, *Superalloys 1996* (TMS AIMA, 1996) 35-43.

Harada H. 2002, ISIJ.3 (2002) 9-15.

Koizumi Y., T. Kobayashi, T. Yokokawa, H. Harada, Y. Aoki, M. Arai, S. Masaki, and K. Chikugo, 2001, *Proc. of 2nd International Symposium on High-Temperature Materials 2001*, Tsukuba, Japan (2001) 30-31.

Zhang J.X., T. Murakumo, Y. Koizumi, T. Kobayashi, H. Harada, and S. Masaki Jr., 2002, *Metallurgical and Materials Transactions A*, 33A, Dec. (2002) 3741-3746.

Yokokawa T., M. Osawa, K. Nishida, Y. Koizumi, T. Kobayashi, and H. Harada, 2002, *Japan Inst. Metals*, 66 (2002) 873-876.

Hino T., T. Kobayashi, Y. Koizumi, H. Harada, and T. Yamagata, 2000, *Superalloys 2000* (TMS AIMA,) 729-736.

Mackay R.A. and L.J. Ebert, 1984, *Superalloys 1984* (TMS AIMA, 1984) 135-144.

Caron P. and T. Khan, 1983, *Mater. Sci. Eng.* 61 (1983) 173-184.

Nabarro F.R.N. and H.L. de Villiers, 1995, The Physics of Creep, (Taylor and Francis, London, 1995) 85-88.